MULTIBODY DYNAMICS 2005, ECCOMAS Thematic Conference
J.M. Goicolea, J. Cuadrado, J.C. García Orden (eds.)
Madrid, Spain, 21–24 June 2005

ENERGY CONSERVING MASTER-SLAVE ALGORITHM FOR GEOMETRICALLY EXACT 3D BEAMS WITH SLIDING JOINTS

José J Muñoz* **and Gordan Jelenić***

*Division of Engineering, King's College London.
Strand, London WC2R 2LS, UK
e-mail: jose.munoz@kcl.ac.uk
* Department of Civil Engineering, University of Rijeka.
V.C. Emina 5, Rijeka, Croatia
e-mail: gordan@gradri.hr

Keywords: master-slave method, conserving time-integration, sliding, large rotations, beams

Abstract. *Contact problems are usually analysed by adding constraint equations to the equilibrium equations of an unconstrained problem. This can be performed by resorting to Lagrange multipliers or penalty methods, or a combination of both (augmented Lagrange method). In order to avoid the time-integration of the differential–algebraic system of equations, we will use the master-slave approach, where the contact conditions are embedded into the equilibrium equations. These can be then integrated using the standard methods employed for unconstrained systems. However, any conservation properties of the algorithms as applied to the unconstrained system may not carry over to the modified master–slave equations with sliding joints.*

The description of the master-slave approach for sliding conditions in 3D beams has been reported in [16]. We will extend this work by writing the master-slave relationship in the incremental form, and then constructing robust conserving time-integration methods for the same kind of problems. It is shown in the paper that, in the present master–slave context, the simultaneous conservation of energy and momenta without violating the sliding conditions is not possible. As a result, we propose an energy conserving algorithm which satisfies the sliding kinematic conditions exactly. Particular situations where contact transition occurs are treated in detail and analysed in the numerical examples.

We note that the approach is applicable to general problems of 3D elastodynamics. In this case, the rotational degrees of freedom are not present, and therefore the related complexities are avoided.

1 INTRODUCTION

Although the study of contact mechanics has attracted great attention in the literature, no accepted optimal method exists for its treatment and it still stands as a challenging field. Most of the works employ two basic routes to solve the contact problem: Lagrange multipliers and the penalty method [3, 4, 22] (or alternatively, augmented Lagrangian, which is a combination of both). However, the former leads to differential-algebraic equations in dynamics, whereas the latter depends on a suitable choice of the penalty parameter and only approximates the contact conditions.

In this paper we develop an alternative method, the master–slave approach, in order to analyse permanent sliding contact of beams. The essence of the method lies in using the relative coordinates (*released displacements*) of the node in contact (*slave node*) with respect to a set of contacted nodes (*master nodes* in a *master element*). The method uses a minimum set of degrees of freedom, and preserves the differential character of the resulting equilibrium equations. We note that the master–slave approach has strong similarities with projection methods [3], joint coordinates in [10], or constraint elimination [22]. However, in our approach, the master–slave relationship is used in the construction of the equilibrium equations, but the global coordinates and velocities are retained in the unmodified time-integration strategy.

Penalty methods or augmented Lagrangian in conjunction with conserving algorithms can be found for instance in [1, 11] in the context of general elastodynamics, and in [2] for 3D beams. On the other hand, the master-slave approach has been used in node-on-node contact for beams with joints in [5, 6, 13], and adapted to conserving algorithms in [8]. An extension of the method for node-on-element contact for sliding joints has been introduced in [16], and a similar technique to the node-on-element master-slave approach has been recently used in [12] in the context of a 2D spring onto a rod, although no reference to conserving time-integrators was done. We will here extend the work in [16] by designing an energy-conserving algorithm for beams with sliding spherical joints. The underlying algorithm is based on the energy-momentum conserving algorithm for geometrically exact 3D beams developed by Simo et al. [20]. We show that the sliding contact conditions impose some restrictions in the conservation of momenta, and that the satisfaction of the contact constrains and the conservation of energy and angular momentum is not possible. As a result, we concentrate on the conservation of energy. Momentum-conserving algorithms for sliding joints within the master-slave approach can be found in [15], where non-released rotations, and joints with dependent released degrees of freedom as the screw joint and the rack-and-pinion joint are also modelled.

The outline of the paper is as follows. We will first briefly describe the underlying beam kinematics and the energy-momentum conserving scheme in Section 2. The derivation of the master-slave relationship in incremental form, needed for this kind of algorithm is introduced in Section 3. Section 4 describes the topology of the coupling element that encapsulates the master and released variables upon the finite element discretisation. The analysis of the conserving properties is studied in Section 5. Cases where the contact point moves to an adjacent element are investigated in Section 6. A set of numerical examples are given in Section 7, and finally, the performance and properties of the proposed algorithm are discussed in Section 8.

2 ENERGY-MOMENTUM ALGORITHM FOR GEOMETRICALLY EXACT BEAMS

2.1 Geometrically exact beam theory

We will first briefly describe the geometrically exact beam theory. The reader is referred to [18, 19] for a more complete exposition of the theory. We will consider a homogeneous

undeformed straight beam with length L in the reference initial configuration. Let us denote by $X \in [0, L]$ the arc-length coordinate of the point in the centroid axis of this undeformed beam, and by $\boldsymbol{e}_i, i = 1, 2, 3$ a spatially fixed triad. At each time $t \in \mathbb{R}_+$, the deformed beam is described via the following two maps: (i) the position vector of the centroid axis $\boldsymbol{r}(X, t) : [0, L] \times \mathbb{R}_+ \to \mathbb{R}^3$ and (ii) the orientation of the undeformable cross-section $\boldsymbol{\Lambda}(X, t) : [0, L] \times \mathbb{R}_+ \to SO(3)$, where $SO(3)$ is the special orthogonal group, i.e. $SO(3) = \{\boldsymbol{\Lambda} | \det \boldsymbol{\Lambda} = +1, \boldsymbol{\Lambda}^{-1} = \boldsymbol{\Lambda}^{\mathrm{T}}\}$. Let us also define the moving triad $\mathbf{g}_i(X, t), i = 1, 2, 3$ as attached to the cross section. The initial configuration is such that $\mathbf{g}_1(X, 0) \equiv \boldsymbol{e}_1$, and matrix $\boldsymbol{\Lambda}(X, t)$ rotates $\mathbf{g}_i(X, t)$ as follows: $\mathbf{g}_i(X, t) = \boldsymbol{\Lambda}(X, t)\boldsymbol{e}_i$. We will denote by $\boldsymbol{G}_i(X)$ the triad $\mathbf{g}(X, t)$ in the initial configuration, i.e. $\boldsymbol{G}_i(X) = \mathbf{g}_i(X, 0)$.

With this definitions at hand, it can be deduced that $\boldsymbol{\Gamma} = \boldsymbol{\Lambda}^{\mathrm{T}}\boldsymbol{r}' - \boldsymbol{G}_1$ and $\boldsymbol{K}$ are the material strain measures, conjugate to the axial and rotational material stress resultants $\boldsymbol{N}$ and $\boldsymbol{M}$, respectively [19]. (Here and henceforth the dash symbol $(')$ denotes differentiation with respect to the arc-length parameter X.) The vector $\boldsymbol{K}$ is the material curvature, and is such that $\boldsymbol{\Lambda}' = \boldsymbol{\Lambda}\widehat{\boldsymbol{K}}$, where a hat $(\widehat{\bullet})$ onto a vector $\boldsymbol{a} \in \mathbb{R}^3$ denotes a skew-symmetric matrix such that $\widehat{\boldsymbol{a}}\boldsymbol{b}$ is the vector product $\boldsymbol{a} \times \boldsymbol{b} = -\widehat{\boldsymbol{b}}\boldsymbol{a}$.

In addition, we introduce the material tensor of inertia $\mathbf{J} = diag[I_X \;\; I_Y \;\; I_X + I_Y]$, and the material angular velocity $\boldsymbol{W}$ such that $\dot{\boldsymbol{\Lambda}} = \boldsymbol{\Lambda}\widehat{\boldsymbol{W}}$, where the dot $\dot{()}$ stands for time differentiation. With this notation, and the assumption of undeformability of the cross-section, the total strain and kinetic energy of the beam can be written as [20],

$$\begin{aligned} V_{int} &= \frac{1}{2}\int_L (\boldsymbol{N} \cdot \boldsymbol{\Gamma} + \boldsymbol{M} \cdot \boldsymbol{K})\, dX, \\ T &= \frac{1}{2}\int_L \rho\,(A\dot{\boldsymbol{r}} \cdot \dot{\boldsymbol{r}} + \boldsymbol{W} \cdot \mathbf{J}\boldsymbol{W})\, dX, \end{aligned} \tag{1}$$

where A and ρ are the cross-section area and the density of the beam, respectively, and the material is assumed to be linearly elastic. The total energy E of the beam is obtained from (1) as $E = V_{int} + T - W_{ext}$, with W_{ext} the work done by the external loads.

Applying the kinematic constraints of the geometrically beam theory to the three-dimensional continua [19], the following differential beam equilibrium equations can be derived:

$$\begin{aligned} \frac{d}{dt}(\rho A\dot{\boldsymbol{r}}) &= (\boldsymbol{\Lambda}\mathbf{N})' + \mathbf{n}_{ext}, \\ \frac{d}{dt}(\boldsymbol{\Lambda}\mathbf{J}\boldsymbol{W}) &= (\boldsymbol{\Lambda}\mathbf{M})' + \widehat{\boldsymbol{r}}'\boldsymbol{\Lambda}\mathbf{N} + \mathbf{m}_{ext}. \end{aligned}$$

Here $\mathbf{n}_{ext}$ and $\mathbf{m}_{ext}$ are the distributed external force and torque vectors, respectively. From these equations, it can be verified that, for conservative external loads, the variation of the total energy is zero, i.e. $\delta E = \delta V_{int} + \delta T - \delta W_{ext} = 0$. In addition, the vectors of *linear* and *angular* momenta, defined by

$$\begin{aligned} \boldsymbol{L} &= \int_L \rho A\dot{\boldsymbol{r}}\, dX, \\ \boldsymbol{\Pi} &= \int_L \rho\,(A\widehat{\boldsymbol{r}}\dot{\boldsymbol{r}} + \boldsymbol{\Lambda}\mathbf{J}\boldsymbol{W})\, dX, \end{aligned}$$

are both constant if no external loads exist [20]. We will describe next a spatial- and time-discretisation that algorithmically conserves energy and the vectors of linear and angular momenta.

2.2 Energy-momentum conserving algorithm for unconstrained beams [20]

Let us consider a deformed configuration of a beam at time t_n defined by the position vector $\boldsymbol{r}_n(X)$ and the rotation matrix $\boldsymbol{\Lambda}_n(X)$ at each point of the centroid line, where here and in the remainder of the paper, $\{\bullet\}_n$ denotes quantities computed at time t_n, , and $\{\bullet\}_{n+\frac{1}{2}} = \frac{1}{2}(\{\bullet\}_n + \{\bullet\}_{n+1})$. Let us also introduce the *incremental* displacement $\boldsymbol{u}$ and the tangent-scaled *spatial* and *material* incremental rotation vectors, $\boldsymbol{\omega}$ and $\boldsymbol{\Omega}$ between time-steps t_n and t_{n+1} in the following way,

$$\begin{aligned} \boldsymbol{u} &= \boldsymbol{r}_{n+1} - \boldsymbol{r}_n & (2)\\ \boldsymbol{\Lambda}_{n+1} &= \mathrm{cay}(\boldsymbol{\omega})\boldsymbol{\Lambda}_n = \boldsymbol{\Lambda}_n \mathrm{cay}(\boldsymbol{\Omega}). & (3) \end{aligned}$$

The rotation matrix $\mathrm{cay}(\boldsymbol{\omega}) \in SO(3)$ is the Cayley transformation, defined by,

$$\mathrm{cay}(\boldsymbol{\omega}) = \mathbf{I} + \frac{1}{1+\frac{1}{4}\boldsymbol{\omega}\cdot\boldsymbol{\omega}}\left(\widehat{\boldsymbol{\omega}} + \frac{1}{2}\widehat{\boldsymbol{\omega}}^2\right) = \left(\mathbf{I} - \frac{1}{2}\widehat{\boldsymbol{\omega}}\right)^{-1}\left(\mathbf{I} + \frac{1}{2}\widehat{\boldsymbol{\omega}}\right), \tag{4}$$

where $\boldsymbol{\omega}$ is the tangent-scaled rotation vector such that $\boldsymbol{\omega}/\|\boldsymbol{\omega}\|$ is the unit vector along the fixed axis and $\|\boldsymbol{\omega}\| = 2\tan(\theta/2)$, with θ the rotated angle. Note that from (3) and the fact that $\mathrm{cay}(\boldsymbol{\Omega})\boldsymbol{\Omega} = \boldsymbol{\Omega}$, it follows that $\boldsymbol{\omega} = \boldsymbol{\Lambda}_n\boldsymbol{\Omega} = \boldsymbol{\Lambda}_{n+1}\boldsymbol{\Omega}$. Moreover, by inserting the second expression of cay in (4) into $\boldsymbol{\Lambda}_{n+1} = \mathrm{cay}(\boldsymbol{\omega})\boldsymbol{\Lambda}_n$, and after differentiating with respect to X both sides of $\boldsymbol{\Lambda}_{n+1} = \mathrm{cay}(\boldsymbol{\omega})\boldsymbol{\Lambda}_n$, the following relations can be obtained [7, 14]:

$$\begin{aligned} \boldsymbol{\Lambda}_{n+1} - \boldsymbol{\Lambda}_n &= \widehat{\boldsymbol{\omega}}\boldsymbol{\Lambda}_{n+\frac{1}{2}} \\ \boldsymbol{K}_{n+1} &= \boldsymbol{K}_n + \boldsymbol{\Lambda}_n^{\mathrm{T}}\mathbf{S}(\boldsymbol{\omega})^{-\mathrm{T}}\boldsymbol{\omega}', \end{aligned} \tag{5}$$

where $\mathbf{S}(\boldsymbol{\omega})^{-1} = \frac{1}{1+\frac{1}{4}\boldsymbol{\omega}\cdot\boldsymbol{\omega}}\left(\mathbf{I} + \frac{1}{2}\widehat{\boldsymbol{\omega}}\right)$.

We will interpolate the incremental quantities $\boldsymbol{u}$ and $\boldsymbol{\omega}$ by using a set of nodal Lagrangian functions I^i and a set of nodal values as follows (summation over repeated indices forming a superscript–subscript pair is understood):

$$\boldsymbol{p}^h = \left\{ \begin{array}{c} \boldsymbol{u}^h(X) \\ \boldsymbol{\omega}^h(X) \end{array} \right\} = I^i(X)\boldsymbol{p}_i. \tag{6}$$

The vectors $\boldsymbol{p}_i^{\mathrm{T}} = \{\boldsymbol{u}_i{}^{\mathrm{T}}\ \boldsymbol{\omega}_i{}^{\mathrm{T}}\}$, $i = 1, \ldots, N_I$ are the vectors of nodal displacements and tangent-scaled rotations, and N_I is the number of nodes of element I. We point out that the functions I^i satisfy the completeness condition $\sum_{i=1}^{N_I} I^i(X) = 1$. By using the following time-stepping discretisation,

$$\dot{\boldsymbol{r}}_{n+\frac{1}{2}} = \frac{\dot{\boldsymbol{r}}_{n+1} + \dot{\boldsymbol{r}}_n}{2} = \frac{\boldsymbol{u}}{\Delta t} \quad , \quad \mathbf{W}_{n+\frac{1}{2}} = \frac{\mathbf{W}_{n+1} + \mathbf{W}_n}{2} = \frac{\boldsymbol{\Omega}}{\Delta t}, \tag{7}$$

definitions (1) and (6), and making use of (5), it is possible to write the increment of energy $\Delta E = E_{n+1} - E_n$ of an element I over a time step Δt as

$$\Delta E = \Delta T + \Delta V_{int} - \Delta V_{ext} = \boldsymbol{p}^I \cdot \boldsymbol{g}^I, \tag{8}$$

where $\boldsymbol{p}^{I\,\mathrm{T}} = \{\boldsymbol{p}_1^{I\,\mathrm{T}} \dots \boldsymbol{p}_{N_I}^{I\,\mathrm{T}}\}$ is the elemental vector of incremental kinematics with dimensions $6 \times N_I$. Each nodal component of the elemental load vector $\boldsymbol{g}^{I\,\mathrm{T}} = \{\boldsymbol{g}^{I,1\,\mathrm{T}} \dots \boldsymbol{g}^{I,N_I\,\mathrm{T}}\}$ can be split in its dynamic, elastic and external parts, respectively, given by,

$$\begin{aligned}
\boldsymbol{g}_d^{I,i} &= \frac{1}{\Delta t}\int_L \rho I^i \left\{ \begin{array}{c} \dot{\boldsymbol{u}} \\ \mathbf{j}_{n+1}\mathbf{w}_{n+1} - \mathbf{j}_n\mathbf{w}_n \end{array} \right\} dX, \\
\boldsymbol{g}_v^{I,i} &= \int_L \left[\begin{array}{cc} I^{i\prime}\mathbf{I} & \mathbf{0} \\ -I^i\widehat{\boldsymbol{r}}'_{n+\frac{1}{2}} & I^{i\prime}\mathbf{I} \end{array} \right] \left\{ \begin{array}{c} \boldsymbol{\Lambda}_{n+\frac{1}{2}}\boldsymbol{N}_{n+\frac{1}{2}} \\ \mathbf{S}(\boldsymbol{\omega})^{-1}\boldsymbol{\Lambda}_n\boldsymbol{M}_{n+\frac{1}{2}} \end{array} \right\} dX, \\
\boldsymbol{g}_e^{I,i} &= -\int_L \left\{ \begin{array}{c} I^i\bar{\mathbf{n}} \\ \mathbf{0} \end{array} \right\} dX.
\end{aligned} \tag{9}$$

Here, $\mathbf{j} = \boldsymbol{\Lambda}\mathbf{J}\boldsymbol{\Lambda}^{\mathrm{T}}$ and $\mathbf{w} = \boldsymbol{\Lambda}\mathbf{W}$ are the spatial counterparts of $\mathbf{J}$ and $\mathbf{W}$, respectively. When considering a single element, the equation $\Delta E = 0$ should be satisfied for arbitrary incremental kinematics, which leads to the following system of non-linear equations:

$$\boldsymbol{g}^{I,i} = \mathbf{0}, \quad i = 1, \dots, N_I. \tag{10}$$

For multi-element analysis, a similar system can be obtained after setting ΔE for the whole model, which is equivalent to the standard assembly of all the elemental load vectors $\boldsymbol{g}^{I\,\mathrm{T}} = \{\boldsymbol{g}^{I,1\,\mathrm{T}} \ \dots \ \boldsymbol{g}^{I,N_I\,\mathrm{T}}\}$. The resulting algorithm is energy- (by construction) and momentum-conserving, as demonstrated in [20]. Note that we have considered only the conservative spatial external force loads in order to simplify the forthcoming expressions (constant external moments are not conservative). Side effects of the interpolation used in this formulation are studied in [9] and an alternative formulation, which is free of these effects, is presented in [15].

3 INCREMENTAL MASTER-SLAVE RELATIONSHIP FOR TRANSLATIONS

Let us consider a (slave) element A with a node sliding onto a (master) element B (see Figure 1). We will take the end node N_A as the sliding node in order to ease the forthcoming notation. The contact points on element B are denoted by $\boldsymbol{r}_{X_n} = \boldsymbol{r}(X_n, t_n)$ and $\boldsymbol{r}_{X_{n+1}} = \boldsymbol{r}(X_{n+1}, t_{n+1})$. We will confine our attention to a situation where all the rotations of the slave node are fully released (spherical joint) and where $\boldsymbol{r}_{X_n}$ and $\boldsymbol{r}_{X_{n+1}}$ are located in the same master element. Situations where the contact point $\boldsymbol{r}_{n+1}$ is located in an adjacent element will be studied in Section 6.

Using the Lagrangian nodal interpolating functions I^j on the master element B, the sliding kinematic conditions are written as follows:

$$\begin{aligned}
&\text{Time } t_n: \quad \boldsymbol{r}_{N_A,n} = \boldsymbol{r}_{X_n} = I^j_{X_n}\boldsymbol{r}_{j,n} \\
&\text{Time } t_{n+1}: \quad \boldsymbol{r}_{N_A,n+1} = \boldsymbol{r}_{X_{n+1}} = I^j_{X_{n+1}}\boldsymbol{r}_{j,n+1}
\end{aligned} \tag{11}$$

with $\boldsymbol{r}_{N_A,n} = \boldsymbol{r}(X_{N_A}, t_n)$, $\boldsymbol{r}_{N_A,n+1} = \boldsymbol{r}(X_{N_A}, t_{n+1})$, $I^j_{X_n} = I^j(X_n)$, and $I^j_{X_{n+1}} = I^j(X_{n+1})$. Figure 2 illustrates the position of the contact point in the two sliding situations mentioned

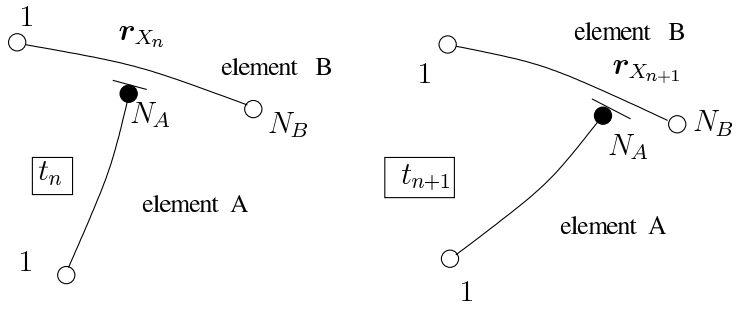

Figure 1: Simplified model of a sliding node. Master and slave nodes are represented by the symbols $\circ$ and $\bullet$, respectively.

above by representing the deformed configurations where no horizonal displacements of the master nodes exist. In this case, the x axis of the figure is representative of the arc-length coordinate X. The deformed configuration at a mid-time $t_{n+\frac{1}{2}}$, which for the master nodes is given by $\boldsymbol{r}_{n+\frac{1}{2}} = I^j \boldsymbol{r}_{j,n+\frac{1}{2}}$, is also depicted in the figure.

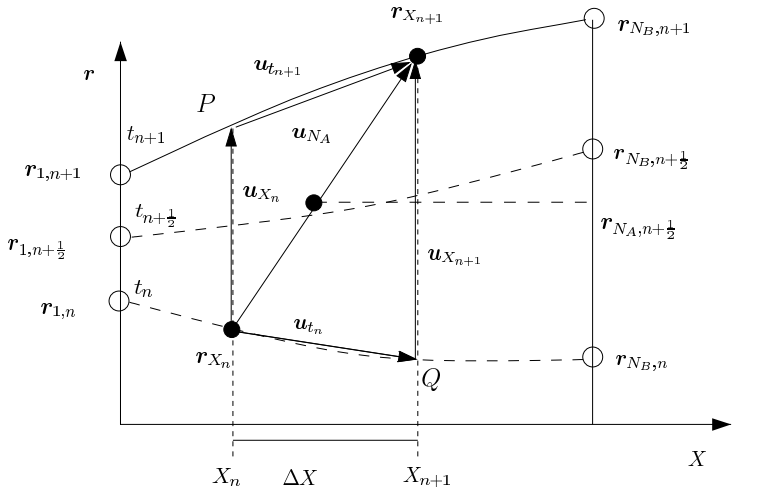

Figure 2: Translational increments over one time-step within one element

Note first that two different paths from $\boldsymbol{r}_{X_n}$ to $\boldsymbol{r}_{X_{n+1}}$ can be distinguished in Figure 2, one through point P and another through point Q. We will weight both routes via a parameter γ, which leads to the following general expression of the incremental slave displacement:

$$\begin{aligned} \boldsymbol{u}_{N_A} &= (1-\gamma)\left(\boldsymbol{u}_{t_n} + \boldsymbol{u}_{X_{n+1}}\right) + \gamma\left(\boldsymbol{u}_{X_n} + \boldsymbol{u}_{t_{n+1}}\right) \\ &= \left((1-\gamma)\boldsymbol{u}_{t_n} + \gamma\boldsymbol{u}_{t_{n+1}}\right) + \left(\gamma\boldsymbol{u}_{X_n} + (1-\gamma)\boldsymbol{u}_{X_{n+1}}\right), \end{aligned} \tag{12}$$

where the meaning of $\boldsymbol{u}_{t_n}$, $\boldsymbol{u}_{t_{n+1}}$, $\boldsymbol{u}_{X_n}$ and $\boldsymbol{u}_{X_{n+1}}$ is also illustrated in Figure 2, and defined as follows:

$$\begin{aligned} \boldsymbol{u}_{t_n} &= \Delta I^j_X \boldsymbol{r}_{j,n}, & \boldsymbol{u}_{X_n} &= I^j_{X_n} \boldsymbol{u}_j, \\ \boldsymbol{u}_{t_{n+1}} &= \Delta I^j_X \boldsymbol{r}_{j,n+1}, & \boldsymbol{u}_{X_{n+1}} &= I^j_{X_{n+1}} \boldsymbol{u}_j, \end{aligned} \tag{13}$$

with $\Delta I^j_X = I^j_{X_{n+1}} - I^j_{X_n}$. For $\gamma = 0$ and $\gamma = 1$ the paths via points Q and P are recovered, respectively. Also, by setting

$$\begin{aligned} I^j_{X\gamma} &= I^j_{X_n}\gamma + I^j_{X_{n+1}}(1-\gamma), \\ \boldsymbol{u}_{n(1-\gamma)} &= (1-\gamma)\boldsymbol{u}_{t_n} + \gamma\boldsymbol{u}_{t_{n+1}}, \end{aligned} \tag{14}$$

we can recast (12) as,

$$\boldsymbol{u}_{N_A} \;=\; \boldsymbol{u}_{n(1-\gamma)} + I^j_{X\gamma}\boldsymbol{u}_j. \tag{15}$$

Let us also introduce the (material) vector of *released* incremental translations $\boldsymbol{u}_R{}^{\mathrm{T}} = \{\Delta X\ 0\ 0\ \}$ which allows us to express the increment of the contact-arc length coordinate as $\Delta X = \boldsymbol{u}_R \cdot \boldsymbol{G}_R$, with $\boldsymbol{G}_R^{\mathrm{T}} = \{1\ 0\ 0\}$ the material unit vector in the direction of the released translation. Hence, the vector $\boldsymbol{u}_{n(1-\gamma)}$ can be written as

$$\boldsymbol{u}_{n(1-\gamma)} = \frac{\boldsymbol{u}_{n(1-\gamma)}}{\Delta X}\Delta X = \frac{1}{\Delta X}(\boldsymbol{u}_{n(1-\gamma)} \otimes \boldsymbol{G}_R)\boldsymbol{u}_R,$$

which inserted into (15) leads to

$$\boldsymbol{u}_{N_A} \;=\; \frac{1}{\Delta X}(\boldsymbol{u}_{n(1-\gamma)} \otimes \boldsymbol{G}_R)\boldsymbol{u}_R + I^j_{X\gamma}\boldsymbol{u}_j. \tag{16}$$

Whenever $\Delta X = 0$, we have $\boldsymbol{u}_{n(1-\gamma)} = \boldsymbol{0}\ \forall\ \gamma \in \mathbb{R}$, and hence $\boldsymbol{u}_{N_A} = \boldsymbol{u}_{X_{n+1}} = \boldsymbol{u}_{X_n}$. If $\Delta X = 0$ corresponds to a non-converged state, the limit case $\Delta X \to 0$ must be used in order to obtain the value of ΔX at equilibrium. For this situation, we can resort to the following result:

$$\lim_{\Delta X\to 0}\frac{\boldsymbol{u}_{n(1-\gamma)}}{\Delta X} = (1-\gamma)\lim_{\Delta X\to 0}\frac{\boldsymbol{u}_{t_n}}{\Delta X} + \gamma\lim_{\Delta X\to 0}\frac{\boldsymbol{u}_{t_{n+1}}}{\Delta X} = (1-\gamma)\boldsymbol{r}'_{t_n} + \gamma\boldsymbol{r}'_{t_{n+1}} = \boldsymbol{r}'_{t_n},$$

and therefore

$$\lim_{\Delta X\to 0}\boldsymbol{u}_{N_A} \;=\; (\boldsymbol{r}'_{t_n} \otimes \boldsymbol{G}_R)\boldsymbol{u}_R + I^j_{X_n}\boldsymbol{u}_j. \tag{17}$$

4 COUPLING ELEMENT DEFINITION

Let us define the vector $\boldsymbol{p}_R^{\mathrm{T}} = \{\boldsymbol{u}_R^{A,N_A\,\mathrm{T}}\ \boldsymbol{\omega}^{A,N_A\,\mathrm{T}}\}$ which contains the incremental released translations and the slave tangent-scaled incremental rotations of node N_A. In addition, we set $\boldsymbol{p}^A_{Rm}$ as the vector that contains the displacements $\boldsymbol{p}_R$, all the displacements of element A, $\boldsymbol{p}^{A\,\mathrm{T}} = \{\boldsymbol{p}^{A,1\,\mathrm{T}}\ \ldots\ \boldsymbol{p}^{A,N_A\,\mathrm{T}}\}$ and the master displacements of element B, i.e.

$$\boldsymbol{p}^A_{Rm}{}^{\mathrm{T}} = \left\{\boldsymbol{p}_R{}^{\mathrm{T}}\ \boldsymbol{p}_1^{A\,\mathrm{T}}\ \ldots \boldsymbol{p}^A_{N_A}{}^{\mathrm{T}}\ \boldsymbol{p}_1^{I\,\mathrm{T}}\ \ldots \boldsymbol{p}^I_{N_B}{}^{\mathrm{T}}\right\}. \tag{18}$$

From equation (16), we can construct the transformation matrix $\mathbf{N}$ that relates $\boldsymbol{p}^A$ and $\boldsymbol{p}^A_{Rm}$ in the following way

$$\boldsymbol{p}^A = \mathbf{N}\boldsymbol{p}^A_{Rm}, \tag{19}$$

where

$$\mathbf{N} = \begin{bmatrix} \bar{\mathbf{0}} & \bar{\mathbf{I}} & \dots & \bar{\mathbf{0}} & \bar{\mathbf{0}} & \bar{\mathbf{0}} & \dots & \bar{\mathbf{0}} \\ \vdots & \vdots & \ddots & \vdots & \vdots & \vdots & \ddots & \vdots \\ \bar{\mathbf{0}} & \bar{\mathbf{0}} & \dots & \bar{\mathbf{I}} & \bar{\mathbf{0}} & \bar{\mathbf{0}} & \dots & \bar{\mathbf{0}} \\ \mathbf{R} & \bar{\mathbf{0}} & \dots & \bar{\mathbf{0}} & \bar{\mathbf{0}} & \bar{\mathbf{I}}_X^1 & \dots & \bar{\mathbf{I}}_X^{N_I} \end{bmatrix}, \tag{20a}$$

and with $\bar{\mathbf{I}}_X^j$ and $\mathbf{R}$ defined as,

$$\begin{aligned} \mathbf{R} &= \begin{bmatrix} \frac{1}{\Delta X}\boldsymbol{u}_{n(1-\gamma)} \otimes \boldsymbol{G}_R & \mathbf{0} \\ \mathbf{0} & \mathbf{I} \end{bmatrix}, \\ \bar{\mathbf{I}}_X^j &= I_{X\gamma}^j \begin{bmatrix} \mathbf{I} & \mathbf{0} \\ \mathbf{0} & \mathbf{0} \end{bmatrix}. \end{aligned} \tag{20b}$$

Here and henceforth, the matrices $\bar{\mathbf{I}}$ and $\bar{\mathbf{0}}$ are the identity and zero 6×6 matrices, respectively. The element with nodal displacements $\boldsymbol{p}_{Rm}^A$ can be regarded as the displacement vector of an extended element that couples the master element B and the slave element A.

5 MASTER–SLAVE ALGORITHMS

5.1 Equilibrium equations

In order to clarify the construction of the equilibrium equations, we will consider the simplified two beam model depicted in Figure 1. The master–slave relationship (19) can be inserted in the energy balance in (8), which leads to

$$\Delta E = \boldsymbol{p}_{Rm}^A \cdot \mathbf{N}^{\mathrm{T}} \boldsymbol{g}^A + \boldsymbol{p}^B \cdot \boldsymbol{g}^B. \tag{21}$$

The product $\boldsymbol{g}_{Rm}^A = \mathbf{N}^{\mathrm{T}} \boldsymbol{g}^A$ is the extended load vector of the coupling element defined previously, conjugate to the displacements $\boldsymbol{p}_{Rm}^A$. From the arbitrariness of the master and released displacements, we obtain a master–slave form of the energy-conserving algorithm for sliding joints. After assembling the load vector of the coupling element and the load vector of element B, the following equilibrium equations are obtained:

$$\begin{aligned} \mathbf{R}^{\mathrm{T}} \boldsymbol{g}^{A,N_A} &= \mathbf{0} & & \\ \boldsymbol{g}^{A,i} &= \mathbf{0} & & i = 1, \dots, N_A - 1 \\ \boldsymbol{g}^{B,j} + \bar{\mathbf{I}}_{X\gamma}^j \boldsymbol{g}^{A,N_A} &= \mathbf{0} & & j = 1, \dots, N_B \end{aligned} \tag{22}$$

When solving this system of non-linear equations, the Jacobian matrix $\mathbf{K}$ of the coupling element load vector $\mathbf{N}^{\mathrm{T}} \boldsymbol{g}^A$ will be required. Its explicit form is given in Appendix A.

5.2 Definition of the algorithms

Let us first note that if the master–slave relationship (12) is satisfied, the extended algorithm inherits the *energy* conserving properties of the original algorithm. Indeed, by inserting the master-slave relationship no approximation is introduced, so the identity $\Delta E = 0$ still holds. However, this is by no means so when it comes to conservation of the angular momentum. It is

shown in Appendix B that the increment of angular momentum over a time-step can be written as:

$$\Delta\boldsymbol{\Pi} = \Delta t \left(\gamma\widehat{\boldsymbol{u}}_{t_{n+1}} - (1-\gamma)\widehat{\boldsymbol{u}}_{t_n}\right) \boldsymbol{g}_f^{A,N_A}, \tag{23}$$

where $\boldsymbol{g}_f^{A,N_A}$ is the translational part of the load vector of node N_A, and $\boldsymbol{u}_{t_n}$ and $\boldsymbol{u}_{t_{n+1}}$ are defined in (13) and in Figure 2. Therefore, the conservation of angular momentum requires the condition $\gamma\widehat{\boldsymbol{u}}_{t_{n+1}} - (1-\gamma)\widehat{\boldsymbol{u}}_{t_n} = \mathbf{0}$, which is equivalent to,

$$\boldsymbol{r}_{N_A,n+\frac{1}{2}} - I^j_{X\gamma}\boldsymbol{r}^B_{j,n+\frac{1}{2}} = \mathbf{0}. \tag{24}$$

In the particular case when $\boldsymbol{r}_j$ has only one variable component, it is possible to obtain a value of γ that satisfies both the kinematic condition (11) and the previous equations. However, for the general three-dimensional case, a choice between conservation of the angular momentum and conservation of energy must be done. Since the violation of the contact conditions spoils the conservation of energy, the clearest choice is to satisfy relation (11). Numerical experiments not shown here also support this choice.

If the sliding contact conditions hold, the error in the identity (24) is in general reduced by setting $\gamma = \frac{1}{2}$. The increment of angular momentum and the slave node position vector will be computed respectively according to equations (23) and (16), with $\gamma = \frac{1}{2}$.

6 CONTACT TRANSITION

We have not yet considered the situation where the two contact points X_{n+1} and X_n lie on two different elements, as depicted in Figure 3. The version of Figure 2 for situations with contact transition is illustrated in Figure 4. Prior to writing a master–slave relationship, however, it is important to note that if the kinematics of both master elements B and C at time t_{n+1} is inserted in the resulting coupling element, the linearisation of the equilibrium equations will couple all three elements A, B and C. This will not only increase the computational cost but also modify the topology of the coupling element in unilateral contact. Therefore, we are interested in relating the incremental kinematics of the slave element A and the last contacted master element C, (but not element B contacted at time t_n). This implies the use of $\gamma = 0$ in equation (16) (path $\boldsymbol{r}_{X_n} - Q - \boldsymbol{r}_{X_{n+1}}$ in Figure 4), which leads to the following expression of the increment of the slave translation:

$$\boldsymbol{u}_{N_A} \;=\; \frac{1}{\Delta X}(\boldsymbol{u}_{t_n} \otimes \mathbf{G}_r)\boldsymbol{u}_R + I^j_{X_{n+1}}\boldsymbol{u}_j. \tag{25}$$

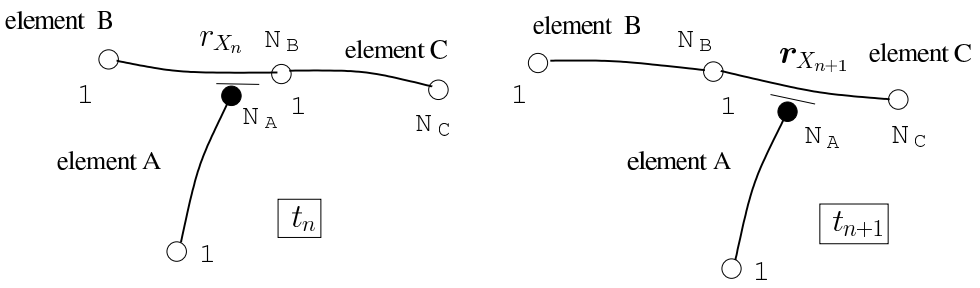

Figure 3: Simplified model for problems with contact transition.

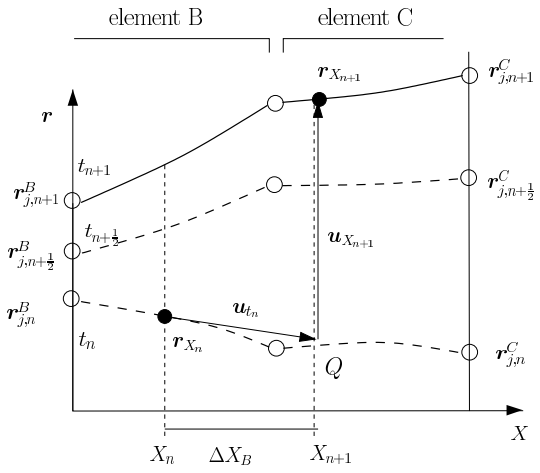

Figure 4: Translational increments over one time-step in the presence of contact transition

Note that now, since $\boldsymbol{r}_{N_A,n}$ and $\boldsymbol{r}_{N_A,n+1}$ belong to two different elements, $\boldsymbol{u}_{t_n}$ is not given by $(13)_1$, but by (see Figure 4)

$$\boldsymbol{u}_{t_n} = I^j_{X_{n+1}} \boldsymbol{r}^C_{j,n} - I^j_{X_n} \boldsymbol{r}^B_{j,n}. \tag{26}$$

The increment of the angular momentum in the present case can be expressed as (see Appendix B, equation (38)):

$$\Delta\boldsymbol{\Pi} = \Delta t \left(\widehat{\boldsymbol{r}}_{N_A,n+\frac{1}{2}} - I^j_{X_{n+1}} \widehat{\boldsymbol{r}}^C_{j,n+\frac{1}{2}} \right) \boldsymbol{g}_f^{A,N_A}. \tag{27}$$

As in the previous section, the condition $\widehat{\boldsymbol{r}}_{N_A,n+\frac{1}{2}} - I^j_{X_{n+1}} \widehat{\boldsymbol{r}}^C_{j,n+\frac{1}{2}} = \boldsymbol{0}$ will be in general in conflict with the kinematic conditions of a sliding joint. These are now written as

$$\begin{aligned} &\text{Time } t_n: \quad \boldsymbol{r}_{N_A,n} = \boldsymbol{r}_{X_n} = I^j_{X_n} \boldsymbol{r}^B_{j,n} \\ &\text{Time } t_{n+1}: \quad \boldsymbol{r}_{N_A,n+1} = \boldsymbol{r}_{X_{n+1}} = I^j_{X_{n+1}} \boldsymbol{r}^C_{j,n+1}. \end{aligned} \tag{28}$$

We can either satisfy the kinematic condition in (28) *or* conserve the angular momentum. Consistently with the choice given in the previous section, the proposed algorithm will be completed by using $\gamma = 0$ and satisfying the sliding kinematic conditions in (28). Note that since the master-slave relationship is exact (in the FE context), the conservation of energy still holds.

The increment of angular momentum is obtained by inserting the kinematic condition (28) into expression (27), which gives rise to

$$\Delta\boldsymbol{\Pi} = \frac{\Delta t}{2} \left(\widehat{\boldsymbol{r}}_{N_A,n} - I^j_{X_{n+1}} \widehat{\boldsymbol{r}}^C_{j,n} \right) \boldsymbol{g}_f^{A,N_A}.$$

Table 1 summarises the properties of the algorithm for the two situations, with and without contact transition.

7 NUMERICAL EXAMPLES

7.1 Free sliding mass

This example models two flexible beams connected through a spherical sliding joint. The initial configuration and the spatial discretisation of the two beams are shown in Figure 5. Except-

	$\Delta E = 0$	$\Delta \boldsymbol{\Pi}$	Sliding condition	γ
No transition	$\surd$	$\frac{\Delta t}{2}\left(\widehat{\boldsymbol{u}}_{t_{n+1}} - \widehat{\boldsymbol{u}}_{t_n}\right)\boldsymbol{g}_f^{A,N_A}$	$\surd$	$\frac{1}{2}$
Contact transition	$\surd$	$-\frac{\Delta t}{2}\widehat{\boldsymbol{u}}_{t_n}\boldsymbol{g}_f^{A,N_A}$	$\surd$	0

Table 1: Summary of conserving and kinematic properties of the proposed algorithm.

ing their lengths, the two beams have identical geometrical and material properties. A mass of 1 kg is attached to beam BM at point M and subjected to an initial velocity $\boldsymbol{v}_0^{\mathrm{T}} = \{0\ -10\ -10\}$. Since there exists no external applied loads, the problem is genuinely energy- and momentum-conserving.

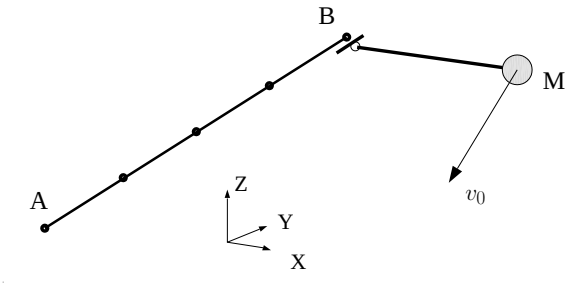

$$A = \left\{ \begin{array}{c} 0.0 \\ 0.0 \\ 0.0 \end{array} \right\}; B = \left\{ \begin{array}{c} 0.0 \\ 3.0 \\ 1.0 \end{array} \right\}; M = \left\{ \begin{array}{c} 1.0 \\ 3.0 \\ 1.0 \end{array} \right\}$$

$$EI_{yy} = EI_{zz} = 20.0$$
$$\rho I_{yy} = \rho I_{zz} = 0.016$$
$$AE = 100.0\ ;\ \rho A = 0.08\ ;\ \nu = 0.3$$

Figure 5: Free sliding mass example.

The simulations are run until the sliding node on beam BM reaches point A. We tested the node-to-element approach to model the sliding joint, together with the the trapezoidal rule as in [16], and the proposed energy-conserving algorithm. A series of deformed configurations at different times using the latter algorithm are depicted in Figure 6.

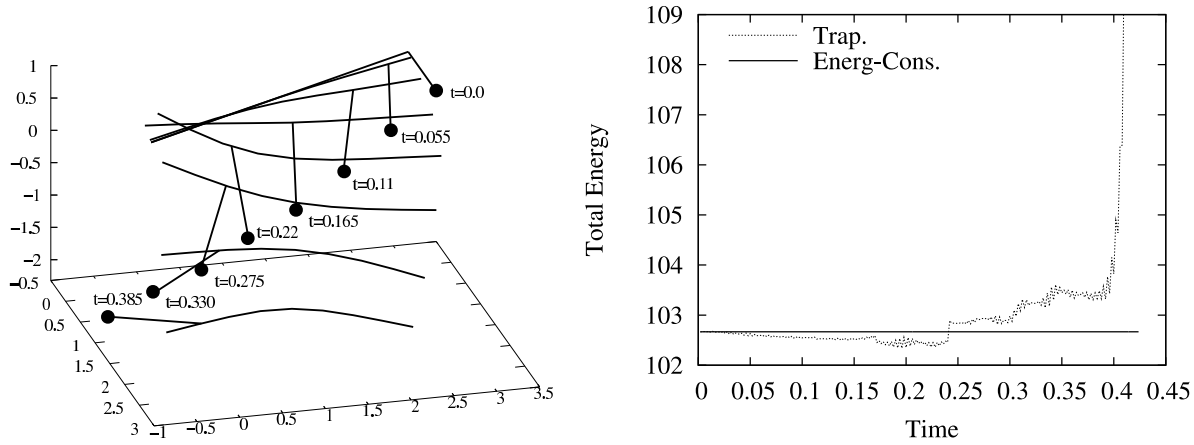

Figure 6: Motion simulation and energy evolution for the free sliding mass problem.

We applied a constant time-step $\Delta t = 0.002$, which allowed the conserving algorithm to terminate the analysis successfully, whereas the widely used trapezoidal rule develops an energy

blow-up and eventually fails to converge before the slave node reaches the end A. The evolution of the total energy in Figure 6 confirms these instabilities.

Figure 7 shows the evolution of the angular momentum. The trapezoidal rule has pronounced oscillations, and although the energy-conserving algorithm does not conserve the angular momentum exactly, its evolution remains stable and apparently bounded. The larger variations are in general always encountered during the transition of the contact point between the elements.

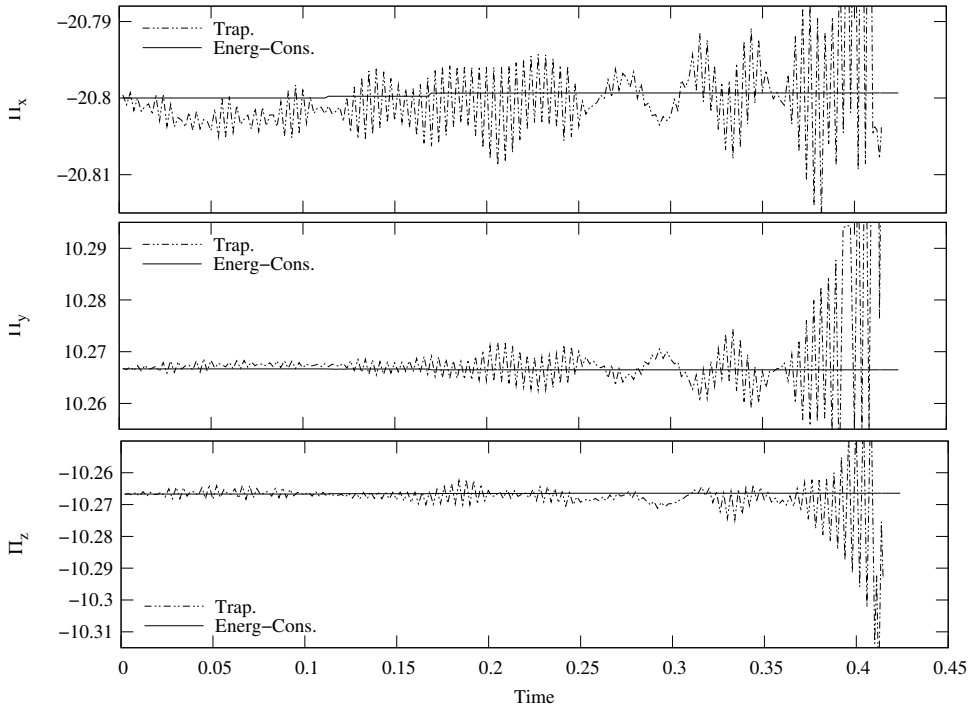

Figure 7: Three components of the angular momentum for the free falling mass example.

7.2 Free rotating arm around a vertical beam

A vertical beam AB clamped at the bottom is connected to an horizontal arm AC via a spherical joint. The material and geometrical properties for the two beams are shown in Figure 8. An initial distributed velocity in the X direction and an angular velocity in the negative Z direction are applied to the arm. Due to the flexibility of the vertical beam, the arm turns around and ascends along AB (see Figure 9).

Both beams have been discretised using four linear elements each, and the same algorithms employed in the previous examples have been used in this problem with a constant time-step size $\Delta t = 0.05$. The energy histories given in Figure 10 show similar tendencies to those of the previous example. The response of the trapezoidal rule has high oscillations in the energy, which affect the history of the released displacement of the slave node along the arm AB (see Figure 10). In addition, from time $t = 0.8$, the trapezoidal rule requires progressive step-halvings in order to converge.

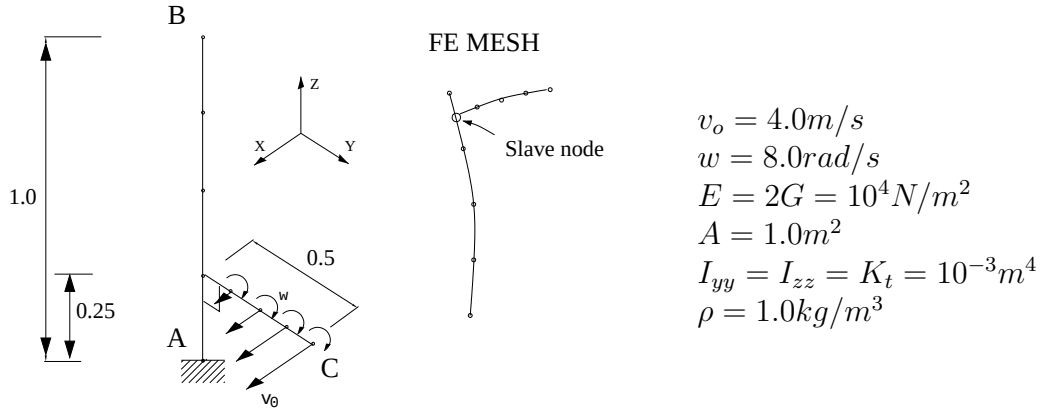

Figure 8: Description of the free rotating beam attached to a spherical joint.

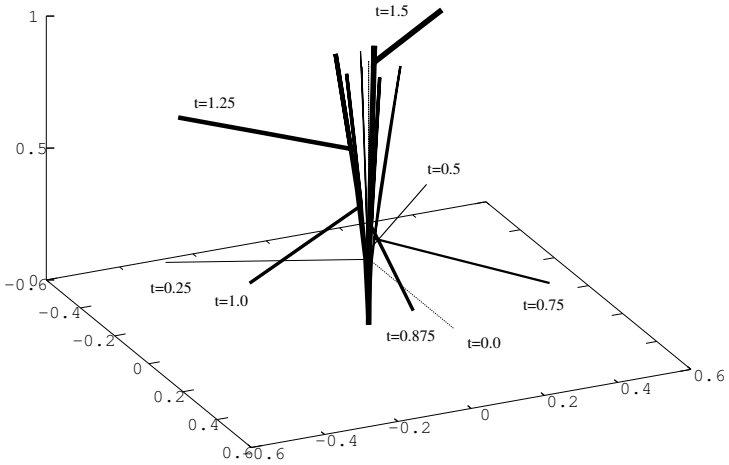

Figure 9: 3D view of the deformed configuration of the free rotating arm with a sliding spherical joint.

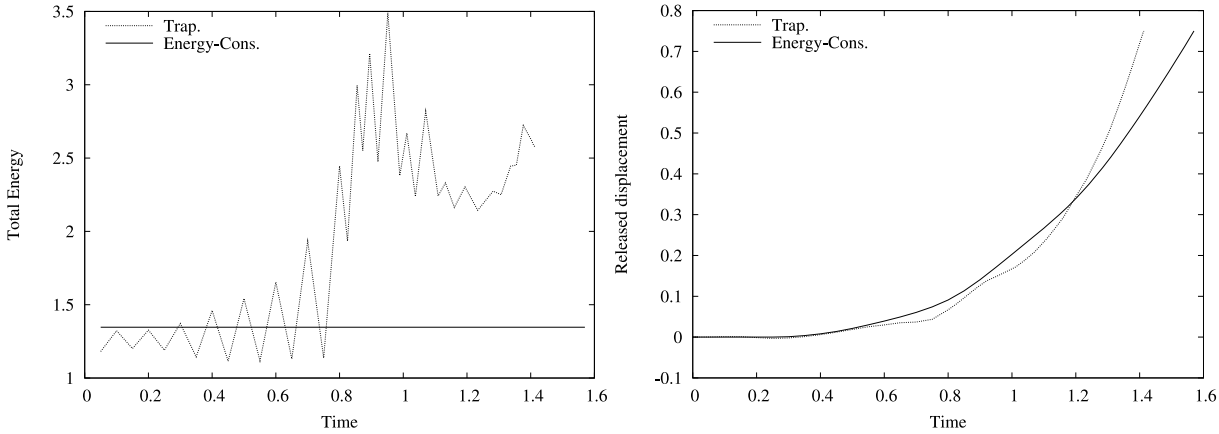

Figure 10: Evolution of the total energy and released displacement for the free rotating arm problem with a sliding spherical joint.

8 DISCUSSION AND CONCLUSIONS

The current paper has extended the master–slave approach in sliding contact analysis by applying to it a robust energy-conserving algorithm. It has been demonstrated that the use of constraint equations can be avoided by embedding the contact conditions in the equilibrium

equations. Special attention has been dedicated to the exact satisfaction of the sliding conditions.

The proposed algorithm conserves the total energy for conserving systems and satisfies exactly the kinematic conditions of a sliding spherical joint. The total energy is still maintained if a contact transition between finite elements is encountered. The numerical results have shown that the variations in the angular momentum remain comparatively small. However, we point out that the conservation of energy would be lost if not all the rotational components at the joint were released. A way of overcoming this problem is proposed in [15], where momentum-conserving algorithms are designed and employed with non-released rotations and a wider type of joints within the framework of strain-invariant interpolation. Numerical experiments not shown here have revealed that discontinuities in the sliding kinematic conditions or conserving properties adversely affect the robustness of the algorithm. For this reason, preservation of the contact conditions has been given a high priority here.

We note that many of the concepts encountered in this paper for the treatment of contact can be transfered and are relevant to general sliding contact conditions in elastodynamics. To the best of our knowledge, its embedding in the conserving algorithms within the master-slave approach has not been explored in the literature. Further work along these lines is currently being carried out.

Finally, let us point out that the transition of contact points along a slideline poses certain difficulties during the solution process, mainly due to the loss of quadratic convergence and discontinuities in the contact forces. These drawbacks affect all the contact techniques mentioned so far. The inclusion of an integral-averaged contacted area within segment-on-segment contact instead of pointwise contact has been proved to palliate part of the problem [17, 21, 22]. However, the mentioned references still make use of Lagrange multipliers for averaging the contact constraints. The combination of this integral-averaging and the master-slave approach looks like a promising research avenue in the study of sliding contact conditions.

A LINEARISATION OF THE COUPLING ELEMENT LOAD VECTOR

Let us split the Jacobian matrix into two parts, one stemming from the linearisation of the elemental load vector $\boldsymbol{g}^A$, and a second one stemming from the linearisation of $\mathbf{N}$:

$$\mathbf{K}_{cp} = \mathbf{N}^{\mathrm{T}}\mathbf{K}_A\mathbf{N}_\delta + \mathbf{K}_N.$$

Matrix $\mathbf{K}_A$ is the elemental Jacobian matrix of the load vector $\boldsymbol{g}^A$, and $\mathbf{N}_\delta$ is the matrix that relates iterative slave displacements and iterative master and released displacements via $\delta\boldsymbol{p}_{N_A} = \mathbf{N}_\delta\delta\boldsymbol{p}_{Rm}$. Its explicit expression is given by [14]:

$$\mathbf{N}_\delta = \begin{bmatrix} \bar{\mathbf{0}} & \bar{\mathbf{I}} & \dots & \bar{\mathbf{0}} & \bar{\mathbf{0}} & \bar{\mathbf{0}} & \dots & \bar{\mathbf{0}} \\ \vdots & \vdots & \ddots & \vdots & \vdots & \vdots & \ddots & \vdots \\ \bar{\mathbf{0}} & \bar{\mathbf{0}} & \dots & \bar{\mathbf{I}} & \bar{\mathbf{0}} & \bar{\mathbf{0}} & \dots & \bar{\mathbf{0}} \\ \mathbf{R}_\delta & \bar{\mathbf{0}} & \dots & \bar{\mathbf{0}} & \bar{\mathbf{0}} & \bar{\mathbf{I}}^1_{X_{n+1}} & \dots & \bar{\mathbf{I}}^{N_B}_{X_{n+1}} \end{bmatrix},$$

with

$$\mathbf{R}_\delta = \begin{bmatrix} \boldsymbol{r}'_{X_{n+1}} \otimes \boldsymbol{G}_R & \mathbf{0} \\ \mathbf{0} & \mathbf{0} \end{bmatrix}, \qquad \text{and} \qquad \bar{\mathbf{I}}^j_{X_{n+1}} = I^j_{X_{n+1}} \begin{bmatrix} \mathbf{I} & \mathbf{0} \\ \mathbf{0} & \mathbf{0} \end{bmatrix}.$$

We will next give the guidelines for deriving matrix $\mathbf{K}_N$, which is generated by the linearisation of $\mathbf{N}$, i.e.:

$$(\delta\mathbf{N}^{\mathrm{T}})\boldsymbol{g}^{A} = \mathbf{K}_{N}\delta\boldsymbol{p}^{A}_{Rm}.$$

By expanding the product $\mathbf{N}^{\mathrm{T}}\boldsymbol{g}^{A}$ and linearising the terms of matrix $\mathbf{N}$, we obtain

$$(\delta\mathbf{N}^{\mathrm{T}})\boldsymbol{g}^{A} \;=\; \left\{ \begin{array}{c} (\delta\mathbf{R}^{\mathrm{T}})\boldsymbol{g}^{A,NA} \\ \mathbf{0}_{6\times N_A} \\ (\delta\bar{\mathbf{I}}^{1}_{X})\boldsymbol{g}^{A,N_A} \\ \vdots \\ (\delta\bar{\mathbf{I}}^{N_I}_{X})\boldsymbol{g}^{A,N_A} \end{array} \right\}, \tag{29a}$$

with

$$\begin{aligned} (\delta\mathbf{R}^{\mathrm{T}})\boldsymbol{g}^{A,N_A} &= \left\{ \begin{array}{c} \delta\left[\frac{1}{\Delta x}\left(\boldsymbol{G}_R\otimes\boldsymbol{u}_{n(1-\gamma)}\right)\right]\boldsymbol{g}^{A,N_A}_{f} \\ \mathbf{0} \end{array} \right\}, \\ (\delta\bar{\mathbf{I}}^{j}_{X})\boldsymbol{g}^{A,N_A} &= \left\{ \begin{array}{c} (\delta I^{j}_{X\gamma})\boldsymbol{g}^{A,N_A}_{f} \\ \mathbf{0} \end{array} \right\}, \end{aligned} \tag{29b}$$

and where $\boldsymbol{g}^{A,N_A}_{f}$ is the translational part of the slave load vector $\boldsymbol{g}^{A,N_A}$. Let us derive some of the required terms in the previous expression:

$$\begin{aligned} \delta\Delta X &= \boldsymbol{G}_R\cdot\delta\boldsymbol{r}_R \\ \delta\boldsymbol{u}_{t_{n+1}} &= \delta(\boldsymbol{r}(X_{n+1},t_{n+1})-\boldsymbol{r}(X_n,t_{n+1})) = \boldsymbol{r}'(X_{n+1},t_{n+1})(\boldsymbol{G}_R\cdot\delta\boldsymbol{r}_R)+\Delta I^{j}\delta\boldsymbol{r}_j \\ \delta\boldsymbol{u}_{t_n} &= \delta\left(\boldsymbol{r}(X_{n+1},t_n)-\boldsymbol{r}(X_n,t_n)\right) = \boldsymbol{r}'(X_{n+1},t_n)(\boldsymbol{G}_R\cdot\delta\boldsymbol{r}_R) \\ \delta(\boldsymbol{u}_{n(1-\gamma)}) &= (1-\gamma)\delta\boldsymbol{u}_{t_n}+\gamma\delta\boldsymbol{u}_{t_{n+1}} = \left([(1-\gamma)\boldsymbol{r}'(X_{t_n},t_n)+\gamma\boldsymbol{r}'(X_{n+1},t_{n+1})]\otimes\boldsymbol{G}_R\right)\delta\boldsymbol{r}_R \\ \delta\left(\frac{1}{\Delta X}\right) &= -\frac{1}{\Delta X^2}(\boldsymbol{G}_R\cdot\delta\boldsymbol{r}_R) \\ \delta I^{j}_{X\gamma} &= (1-\gamma)I'^{j}_{X_{n+1}}(\boldsymbol{G}_R\cdot\delta\boldsymbol{r}_R) \end{aligned}$$

The expression for $(\delta\mathbf{N}^{\mathrm{T}})\boldsymbol{g}^{A}$ can be now completed by inserting these results into (29). This leads to a matrix $\mathbf{K}_N$ such that $(\delta\mathbf{N}^{\mathrm{T}})\boldsymbol{g}^{A} = \mathbf{K}_N\delta\boldsymbol{p}^{A}_{Rm}$, and given by

$$\mathbf{K}_N = \left[\begin{array}{ccc} \mathbf{K}_{RR} & \mathbf{0}_{6\times 6N_A} & \mathbf{K}_{Rm} \\ \mathbf{0}_{6N_A\times 6} & \mathbf{0}_{6N_A\times 6N_A} & \mathbf{0}_{6N_A\times 6N_I} \\ \mathbf{K}_{mR} & \mathbf{0}_{6N_B\times 6N_A} & \mathbf{0}_{6N_B\times 6N_I} \end{array}\right].$$

The explicit forms of $\mathbf{K}_{Rm}$, $\mathbf{K}_{RR}$ and $\mathbf{K}_{mR}$ are as follows:

$$\begin{aligned} \mathbf{K}_{RR} &= \left[\begin{array}{cc} \frac{1}{\Delta X}\left(\left(-\frac{\boldsymbol{u}_{n(1-\gamma)}}{\Delta X}+\boldsymbol{r}'_{X_{n+1},t_n}+\gamma\boldsymbol{u}'_{X_{n+1}}\right)\cdot\boldsymbol{g}^{A,N_A}_{f}\right)\boldsymbol{G}_R\otimes\boldsymbol{G}_R & \mathbf{0} \\ \mathbf{0} & \mathbf{0} \end{array}\right] \\ \mathbf{K}_{Rm} &= \left[\mathbf{K}^{1}_{Rm}\ \ldots\ \mathbf{K}^{N_B}_{Rm}\right] \\ \mathbf{K}^{j}_{Rm} &= \left[\begin{array}{cc} \frac{1}{\Delta X}\left(\boldsymbol{G}_R\otimes\boldsymbol{g}^{A,N_A}_{f}\right)\Delta I^{j}\gamma & \mathbf{0} \\ \mathbf{0} & \mathbf{0} \end{array}\right] \end{aligned}$$

$$\mathbf{K}_{mR} = \begin{bmatrix} \mathbf{K}^1_{mR} \\ \vdots \\ \mathbf{K}^{N_I}_{mR} \end{bmatrix}$$
$$\mathbf{K}^j_{mR} = \begin{bmatrix} I'^j_{X_{n+1}}(1-\gamma)\boldsymbol{g}_f^{A,N_A} & \mathbf{0} \\ \mathbf{0} & \mathbf{0} \end{bmatrix}.$$

B PROOF OF THE CONSERVATION OF MOMENTA

Since we aim to prove the conservation of angular momentum in the absence of applied loads, we will restrict our attention to the case $\boldsymbol{g}_e^{I,i} = \mathbf{0}$, $i = 1, \dots, N_I$, $I = A, B$ or C, in the subsequent derivations.

B.1 No contact transition

By splitting the load vectors into the translational and rotational part, i.e. $\boldsymbol{g}^{I,i} = \{\boldsymbol{g}_f^{I,i}\ \boldsymbol{g}_\phi^{I,i}\}$, the equilibrium equations in (22) for the reduced model shown in Figure 1 are written as

$$\mathbf{R}^{\mathrm{T}}\boldsymbol{g}^{A,N_A} = \mathbf{0} \tag{30a}$$
$$\boldsymbol{g}^{A,i} = \mathbf{0} \qquad i = 1, \dots, N_A - 1 \tag{30b}$$
$$\boldsymbol{g}_f^{B,j} + I^j_{X\gamma}\boldsymbol{g}_f^{A,N_A} = \mathbf{0} \qquad j = 1, \dots, N_B \tag{30c}$$
$$\boldsymbol{g}_\phi^{B,j} = \mathbf{0} \qquad j = 1, \dots, N_B. \tag{30d}$$

Consequently, after adding all the nodal load vectors for both elements, and using equations (30a)-(30d), we get the following preliminary result:

$$\sum_{i=1}^{N_A}\boldsymbol{g}_f^{A,i} + \sum_{j=1}^{N_B}\boldsymbol{g}_f^{B,j} = \boldsymbol{g}_f^{A,N_A} - \underbrace{\left(\sum_{j=1}^{N_B} I^j_{X\gamma}\right)}_{=1}\boldsymbol{g}_f^{A,N_A} = \mathbf{0}, \tag{31a}$$
$$\sum_{i=1}^{N_A}\boldsymbol{g}_\phi^{A,i} + \sum_{j=1}^{N_B}\boldsymbol{g}_\phi^{B,j} = \mathbf{0} + \mathbf{0} = \mathbf{0}, \tag{31b}$$

where use of the completeness conditions of the Lagrangian polynomials $I^j_{X\gamma}$ and ${}^j_{X_{n+1}}$ has been made. The conservation of the total linear momentum $\boldsymbol{L} = \int_L \rho A\dot{\boldsymbol{r}}dX$ can be deduced by noting that from the definitions of load vectors in (9) we have that

$$\Delta\boldsymbol{L} = \int_{L^A+L^B}\rho A\dot{\boldsymbol{u}}dX = \sum_{i=1}^{N_A}\boldsymbol{g}_f^{A,i} + \sum_{j=1}^{N_B}\boldsymbol{g}_f^{B,j} = \mathbf{0},$$

where the last identity follows from equation (31a). In order to ease the forthcoming derivations, let us set $\boldsymbol{\pi} = \rho\mathbf{j}\mathbf{w}$ as the density of local angular momentum. The conservation of the total angular momentum $\boldsymbol{\Pi} = \int_L(\boldsymbol{\pi} + \rho A\widehat{\boldsymbol{r}}\dot{\boldsymbol{r}})dX$ can be demonstrated by first remarking that also from the definitions of the load vectors in (9) and equation (31b) we obtain

$$\frac{1}{\Delta t}\int_{L^A+L^B}\Delta\boldsymbol{\pi}dX - \int_{L^A+L^B}\widehat{\boldsymbol{r}}'_{n+\frac{1}{2}}\boldsymbol{\Lambda}_{n+\frac{1}{2}}\boldsymbol{N}_{n+\frac{1}{2}}dX = \mathbf{0}$$

or using the FE interpolation $\boldsymbol{r}'_{n+\frac{1}{2}} = I^{i'}\boldsymbol{r}^{i}_{n+\frac{1}{2}}$ within each element,

$$\frac{1}{\Delta t}\int_{L^A+L^B}\Delta\boldsymbol{\pi}dX = \sum_{I=A,B}\sum_{i=1}^{N_I}\widehat{\boldsymbol{r}}_{i,n+\frac{1}{2}}\int_{L^I} I^{i'}\boldsymbol{\Lambda}_{n+\frac{1}{2}}\boldsymbol{N}_{n+\frac{1}{2}}dX. \tag{32}$$

On the other hand, the increment of the the angular momentum $\Delta\boldsymbol{\Pi}$ over a time-step is given by,

$$\begin{aligned}\Delta\boldsymbol{\Pi} &= \int_{L^A+L^B}\left(\Delta\boldsymbol{\pi}+\rho A\widehat{\boldsymbol{r}}_{n+1}\dot{\boldsymbol{r}}_{n+1}-\rho A\widehat{\boldsymbol{r}}_{n}\dot{\boldsymbol{r}}_{n}\right)dX\\ &= \int_{L^A+L^B}\Delta\boldsymbol{\pi}dX+\int_{L^A+L^B}\rho A\left(\widehat{\boldsymbol{r}}_{n+\frac{1}{2}}\dot{\boldsymbol{u}}+\widehat{\boldsymbol{u}}\dot{\boldsymbol{r}}_{n+\frac{1}{2}}\right)dX\\ &= \int_{L^A+L^B}\Delta\boldsymbol{\pi}dX+\int_{L^A+L^B}\rho A\widehat{\boldsymbol{r}}_{n+\frac{1}{2}}\dot{\boldsymbol{u}}dX.\end{aligned} \tag{33}$$

where the last result follows from the time-integration mid-point rule (7), i.e. $\widehat{\boldsymbol{u}}\dot{\boldsymbol{r}} = \boldsymbol{0}$. Inserting equation (32) into the first integral of (33) yields

$$\begin{aligned}\Delta\boldsymbol{\Pi} &= \sum_{I=A,B}\sum_{i}^{N_A+N_B}\widehat{\boldsymbol{r}}_{i,n+\frac{1}{2}}\left(\Delta t\int_{L^I} I^{i'}\boldsymbol{\Lambda}_{n+\frac{1}{2}}\boldsymbol{N}_{n+\frac{1}{2}}dX+\int_{L^I}\rho A I^{i}\dot{\boldsymbol{u}}dX\right)\\ &= \Delta t\sum_{I=A,B}\sum_{i=1}^{N_I}\widehat{\boldsymbol{r}}_{i,n+\frac{1}{2}}\boldsymbol{g}_f^{I,i},\end{aligned} \tag{34}$$

where the last step follows by recognising that the term in parentheses is the translational part of $\boldsymbol{g}^i = \boldsymbol{g}^i_d + \boldsymbol{g}^i_v$ in (9). By using the equilibrium equations (30b) and (30c), and the definitions in (13), yields,

$$\Delta\boldsymbol{\Pi} = \Delta t\left(\widehat{\boldsymbol{r}}_{N_A,n+\frac{1}{2}}-\sum_{j}^{N_B}I^{j}_{X\gamma}\widehat{\boldsymbol{r}}_{j,n+\frac{1}{2}}\right)\boldsymbol{g}_f^{A,N_A} = \Delta t\left(\gamma\widehat{\boldsymbol{u}}_{t_{n+1}}-(1-\gamma)\widehat{\boldsymbol{u}}_{t_n}\right)\boldsymbol{g}_f^{A,N_A}$$

It is clear that the kinematic condition $\gamma\boldsymbol{u}_{t_{n+1}}-(1-\gamma)\boldsymbol{u}_{t_n}=\boldsymbol{0}$ makes the algorithm angular momentum conserving.

B.2 Contact transition

We remember that these algorithms use the the value $\gamma = 0$, and therefore, matrix $\bar{\mathbf{I}}^j_X$ is the one in (20b) but with $I^j_{X\gamma} = I^j_{X_{n+1}}$. Let us resort to the reduced problem in Figure 3 which contains elements A, B and C. After performing the nodal assembly, the systems of equations prior and after the introduction of the master-slave relationship $\boldsymbol{p}^A = \mathbf{N}\boldsymbol{p}^A_{Rm}$ are written as

$$
\begin{array}{rl}
\underline{\text{Before m-s}} & \underline{\text{After m-s}} \\
\boldsymbol{g}^{A,N_A} = \boldsymbol{0} & \mathbf{R}^{\mathrm{T}}\boldsymbol{g}^{A,N_A} = \boldsymbol{0}, \\
\boldsymbol{g}^{A,i} = \boldsymbol{0} & \boldsymbol{g}^{A,i} = \boldsymbol{0} \quad , \quad i = 1, \dots, N_A - 1, \\
\boldsymbol{g}^{B,j} = \boldsymbol{0} & \boldsymbol{g}^{B,j} = \boldsymbol{0} \quad , \quad j = 1, \dots, N_B - 1, \\
\boldsymbol{g}_f^{C,j} = \boldsymbol{0} & \boldsymbol{g}_f^{C,j} + I^j_{X_{n+1}} \boldsymbol{g}_f^{A,N_A} = \boldsymbol{0} \quad , \quad j = 2, \dots, N_C, \\
\boldsymbol{g}_\phi^{C,j} = \boldsymbol{0} & \boldsymbol{g}_\phi^{C,j} = \boldsymbol{0} \quad , \quad j = 2, \dots, N_C, \\
\boldsymbol{g}_f^{C,1} + \boldsymbol{g}_f^{B,N_B} = \boldsymbol{0} & \boldsymbol{g}_f^{C,1} + I^1_{X_{n+1}} \boldsymbol{g}_f^{A,N_A} + \boldsymbol{g}_f^{B,N_B} = \boldsymbol{0}, \\
\boldsymbol{g}_\phi^{C,1} + \boldsymbol{g}_\phi^{B,N_B} = \boldsymbol{0} & \boldsymbol{g}_\phi^{C,1} + \boldsymbol{g}_\phi^{B,N_B} = \boldsymbol{0}.
\end{array}
\tag{35}
$$

Let us first derive an equivalent version of equations (31) by adding all the nodal contributions of the load vectors and using the previous equilibrium equations,

$$
\sum_{i=1}^{N_A} \boldsymbol{g}_f^{A,i} + \sum_{j=1}^{N_B} \boldsymbol{g}_f^{B,j} + \sum_{j=1}^{N_C} \boldsymbol{g}_f^{C,j} = \boldsymbol{g}_f^{A,N_A} + \boldsymbol{g}_f^{B,N_B} - \underbrace{\left(\sum_{j=1}^{N_C} I^j_{X_{n+1}} \right)}_{=1} \boldsymbol{g}_f^{A,N_A} - \boldsymbol{g}_f^{B,N_B} = \boldsymbol{0}
$$

$$
\sum_{i=1}^{N} \boldsymbol{g}_\phi^{A,i} + \sum_{j=1}^{N_B} \boldsymbol{g}_\phi^{B,j} + \sum_{j=1}^{N_C} \boldsymbol{g}_\phi^{C,j} = \boldsymbol{0}. \tag{36}
$$

From these relations, and using similar manipulations to Section B.1, it can be then verified that the increment of angular momentum has the same expression as in (34), but with the integral and the sum over the three elements A, B and C, i.e.

$$
\frac{\Delta \boldsymbol{\Pi}}{\Delta t} \;=\; \sum_{I=A,B,C} \sum_{i=1}^{N_I} \widehat{\boldsymbol{r}}_{i,n+\frac{1}{2}} \boldsymbol{g}_f^{I,i}. \tag{37}
$$

Thus, by making use of the equilibrium equations (35), and the fact that $\boldsymbol{r}^B_{N_B,n+\frac{1}{2}} = \boldsymbol{r}^C_{1,n+\frac{1}{2}}$ (this is the common node to elements B and C), the following expression can be derived:

$$
\begin{aligned}
\frac{\Delta \boldsymbol{\Pi}}{\Delta t} \;&=\; \widehat{\boldsymbol{r}}_{N_A,n+\frac{1}{2}} \boldsymbol{g}_f^{A,N_A} + \widehat{\boldsymbol{r}}^B_{N_B,n+\frac{1}{2}} \boldsymbol{g}_f^{B,N_B} - \sum_{j=1}^{N_C} \widehat{\boldsymbol{r}}^C_{j,n+\frac{1}{2}} I^j_{X_{n+1}} \boldsymbol{g}_f^{A,N_A} - \widehat{\boldsymbol{r}}^C_{1,n+\frac{1}{2}} \boldsymbol{g}_f^{B,N_B} \\
&=\; \left(\widehat{\boldsymbol{r}}_{N_A,n+\frac{1}{2}} - \sum_{j=1}^{N_C} I^j_{X_{n+1}} \widehat{\boldsymbol{r}}^C_{j,n+\frac{1}{2}} \right) \boldsymbol{g}_f^{A,N_A},
\end{aligned}
$$

The angular momentum is thus conserved if the kinematic condition $\boldsymbol{r}_{N_A,n+\frac{1}{2}} = I^j_{X_{n+1}} \boldsymbol{r}^C_{j,n+\frac{1}{2}}$ is satisfied. If instead the sliding conditions (28) are imposed, it can be verified that the increment of angular momentum is equal to

$$
\Delta \boldsymbol{\Pi} \;=\; \frac{\Delta t}{2} \left(\widehat{\boldsymbol{r}}_{N_A,n} - I^j_{X_{n+1}} \widehat{\boldsymbol{r}}^C_{j,n} \right) \boldsymbol{g}_f^{A,N_A}. \tag{38}
$$

REFERENCES

[1] F Armero and E Petőcz. Formulation and analysis of conserving algorithms for frictionless dynamic contact/impact problems. *Comp. Meth. Appl. Mech. Engng.*, 158:269–300, 1998.

[2] O Bauchau. On the modeling of prismatic joints in flexible multy-body systems. *Comp. Meth. Appl. Mech. Engng.*, 181:87–105, 2000.

[3] J García de Jalón and E Bayo. *Kinematic and dynamic simulation of multibody systems – the real-time challenge*. Springler-Verlag, New York, 1994.

[4] M A Géradin and A Cardona. *Flexible Multibody Dynamics. A Finite Element Approach.* John Wiley & Sons, 2001.

[5] A Ibrahimbegović and S Mamouri. On rigid components and joint constraints in nonlinear dynamics of flexible multibody systems employing 3D geometrically exact beam model. *Comp. Meth. Appl. Mech. Engng.*, 188:805–831, 2000.

[6] G Jelenić and M A Crisfield. Non-linear master-slave relationships for joints in 3D beams with large rotations. *Comp. Meth. Appl. Mech. Engng.*, 135:211–228, 1996.

[7] G Jelenić and M A Crisfield. Stability and convergence characteristics of conserving algorithms for dynamics of 3D rods. Technical report, Department of Aeronatics, Imperial College, London, 1999.

[8] G Jelenić and M A Crisfield. Dynamic analysis of 3D beams with joints in presence of large rotations. *Comp. Meth. Appl. Mech. Engng.*, 32-33:4195–4230, 2001.

[9] G Jelenić and M A Crisfield. Problems associated with the use of Cayley transform and tangent scaling for conserving energy and momenta in the Reissner-Simo beam theory. *Comm. Num. Meth. Engng.*, 18:711–720, 2002.

[10] W Jerkovsky. The structure of multibody dynamics equations. *J. Guidance and Control*, 1(3):173–182, 1978.

[11] T A Laursen and V Chawla. Desing of energy conserving algorithms for frictionless dynamic contact problems. *Int. J. Num. Meth. Engng.*, 40:863–886, 1997.

[12] H Marjamäki and J Mäkinen. Modelling telescopic boom – The plane case: part I. *Comput. Struct.*, 81:1597–1609, 2003.

[13] J Mitsugi. Direct strain measure for large displacement analyses on hinge connected beam structures. *Comput. Struct.*, 64:509–517, 1997.

[14] J Muñoz. *Finite-element analysis of flexible mechanisms using the master-slave approach with emphasis on the modelling of joints*. PhD thesis, Imperial College London, 2004.

[15] J Muñoz and G Jelenić. Sliding joints in 3D beams: conserving algorithms using the master–slave approach. To be submitted.

[16] J Muñoz and G Jelenić. Sliding contact conditions using the master–slave approach with application on the geometracally non-linear beams. *Int. J. Solids Struct.*, 41:6963–6992, 2004.

[17] M A Puso and T A Laursen. A mortar segment-to-segment contact method for large deformation solid mechanics. *Comp. Meth. Appl. Mech. Engng.*, 93:601–629, 2004.

[18] E Reissner. On one-dimensional large-displacement finite-strain beam theory. *Studies in Applied Mathem.*, 52:87–95, 1973.

[19] J C Simo. A finite strain beam formulation. The three dimensional dynamic problem. Part I. *Comp. Meth. Appl. Mech. Engng.*, 49:55–70, 1985.

[20] J C Simo, N Tarnow, and M Doblare. Non-linear dynamics of three-dimensional rods: exact energy and momentum conserving algorithms. *Int. J. Num. Meth. Engng.*, 38:1431–1473, 1995.

[21] J C Simo, P Wriggers, and R L Taylor. A perturbed Lagrangian formulation for the finite element solution of contact problems. *Comp. Meth. Appl. Mech. Engng.*, 50:163–180, 1985.

[22] P Wriggers. *Computational Contact Mechanics*. Wiley, 2002.